



Spiral Arm Structure: [NII] and [CII] in the Scutum Arm

Bill Langer (JPL-Caltech)

December 6, 2017

Based on:

“Ionized gas in the Scutum spiral arm as traced in [N II] and [C II]”

W. D. Langer, T. Velusamy, P. F. Goldsmith, J. L. Pineda, E. T.

Chambers, G. Sandell, C. Risacher, & K. Jacobs

A&A 607, A59 (2017)



Outline

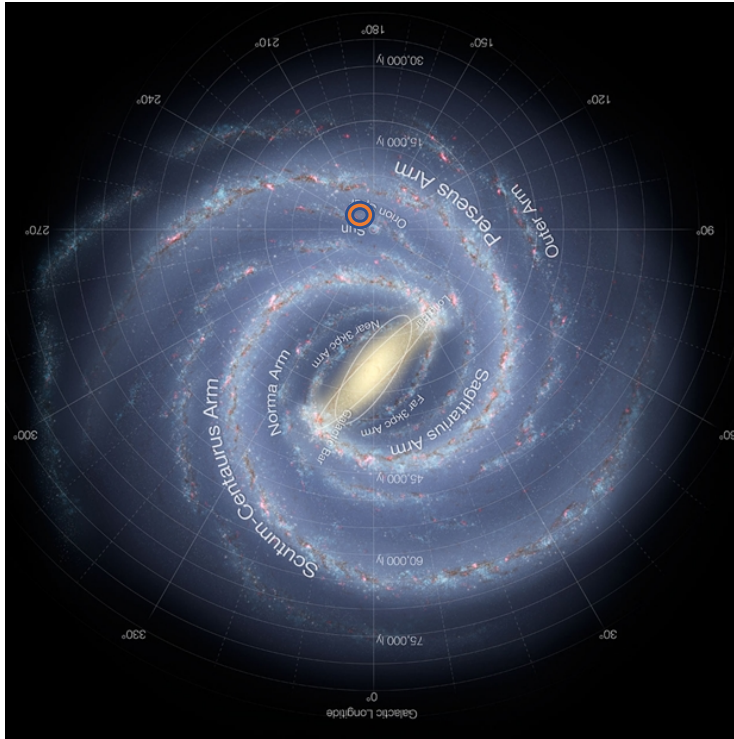
- Intro: Characterizing Spiral Arm Ionized Layers
- Observations: [NII] & [CII] at the Scutum arm
- Results: Properties of the Scutum Arm Ionized Gas
- Discussion: Arm - Interarm Interaction
- Summary



Galactic Spiral Arms - Simple View

THE ASTROPHYSICAL JOURNAL SUPPLEMENT SERIES, 215:1 (9pp), 2014 November

VALLÉE



Artist conception: Robert Hurt (NASA:SSC)

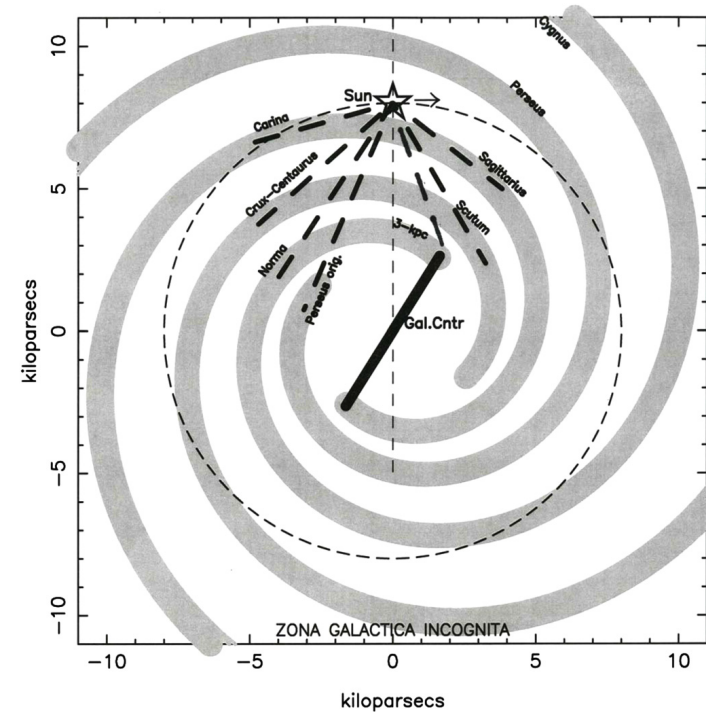
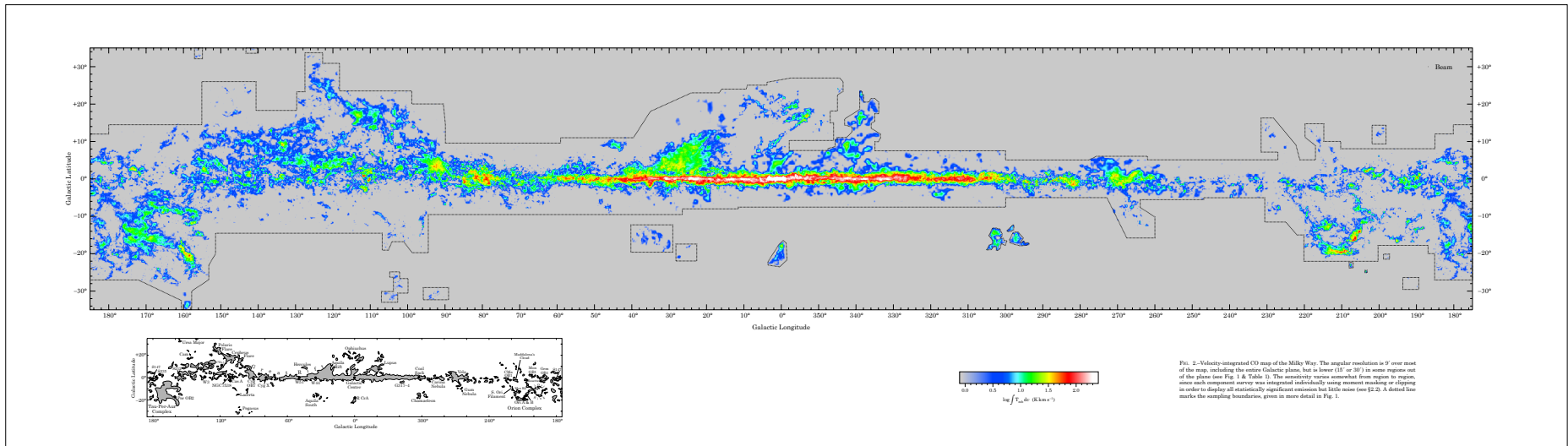


Figure 1. Old galactography. The Sun is shown (open star) at 8 kpc from the Galactic center, with the clockwise Galactic rotation (arrow). Most stars in the Milky Way galaxy are located along four spiral arms (gray). Other components such as clouds, gas, atoms, dust, and cosmic rays are also in there. Approximate arm tangents as seen from the Sun are shown (thick black dashes). The Sun's orbit is shown here as a circle (thin dashes). A rough position for the Galactic bar is shown. Not much is known below the Galactic center, called "Zona Galactica Incognita" a.k.a. "unknown Galactic area" following Vallée (2002; his Figure 2). The Galactic center is at (0, 0) and the distance scale at bottom and to the left follows common conventions.

M. Reid (2014)
 $R_0 = 8.4 \pm 0.6$ kpc
 $Q_0 = 254 \pm 16$ km/s



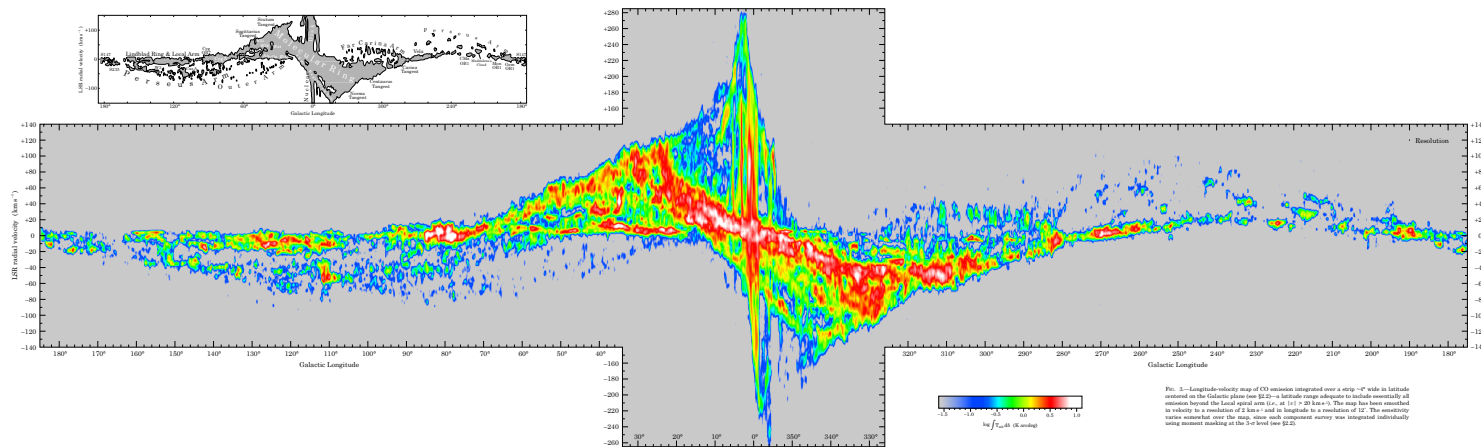
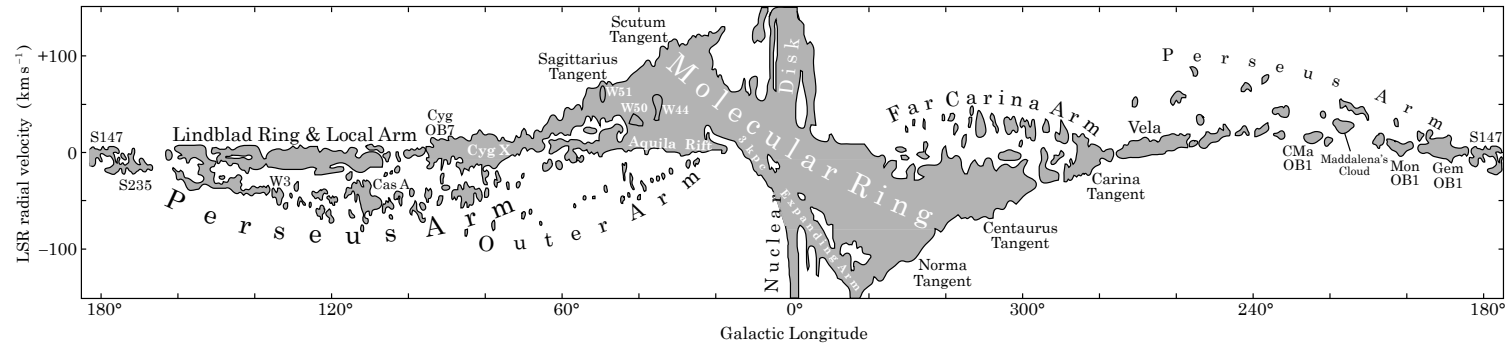
^{12}CO Distribution



Dame et al. (2006) Integrated Intensity Map



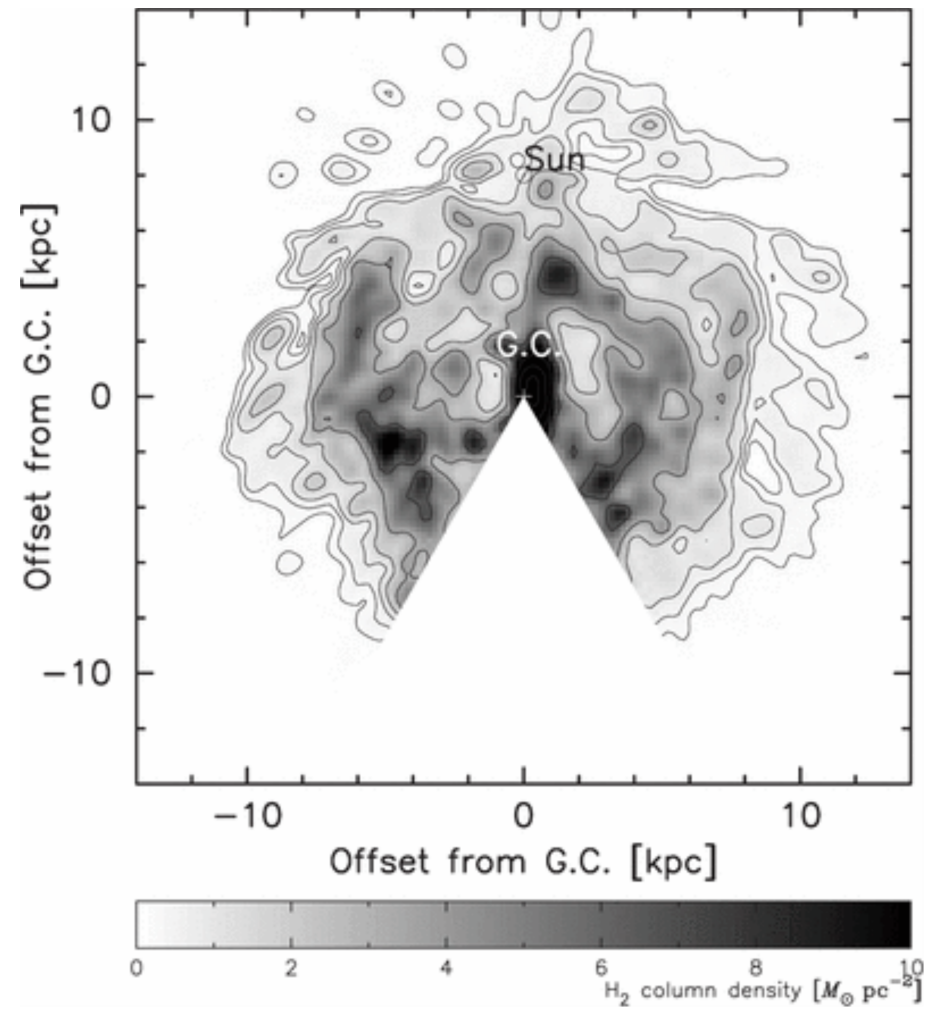
^{12}CO Velocity Distribution



Dame et al. (2006)



H₂ Spiral Arms Traced in CO



H₂ gas in the disk

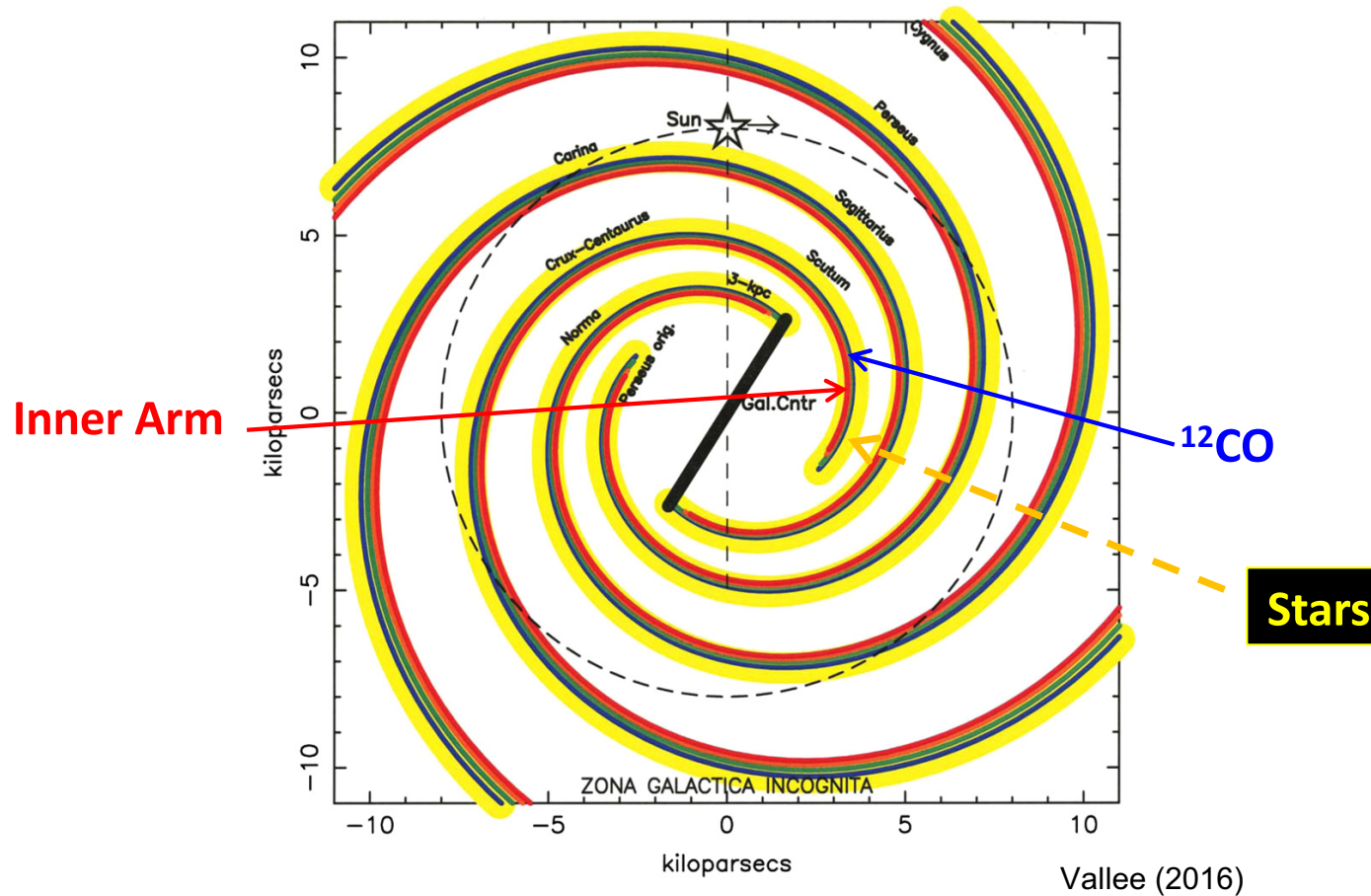
Nakanishi et al. (2006) (based on Dame et al. (2001) CO survey)



Spiral Arm Evolution

THE ASTROPHYSICAL JOURNAL SUPPLEMENT SERIES, 215:1 (9pp), 2014 November

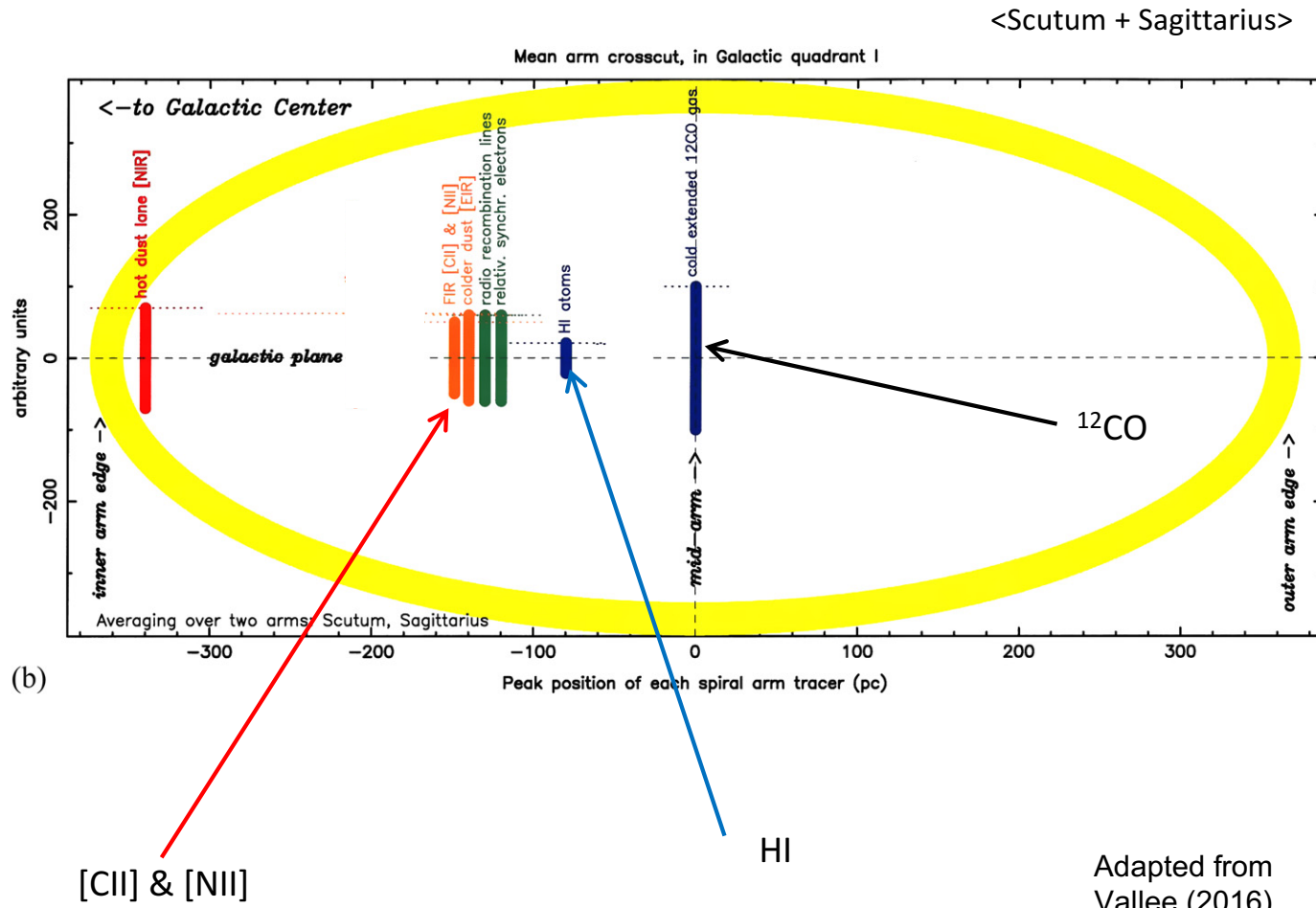
VALLÉE



Spiral arms undergo a phase change from low density ionized gas to dense H₂ clouds, and eventually star formation



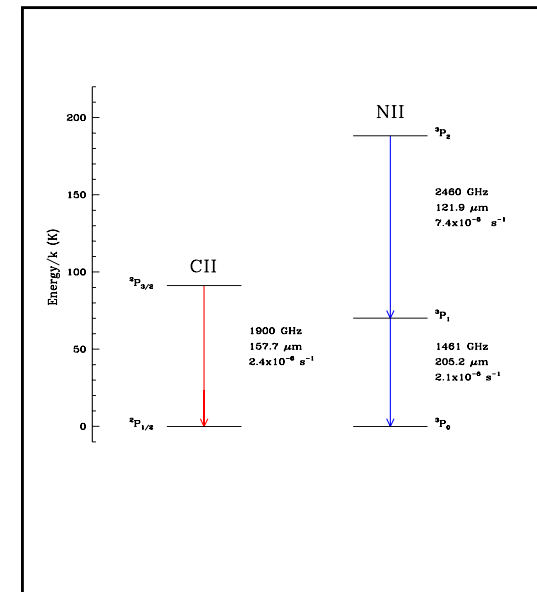
Spiral Arm Tracers vs. Position





Tracing the Ionized Spiral Arm Lanes

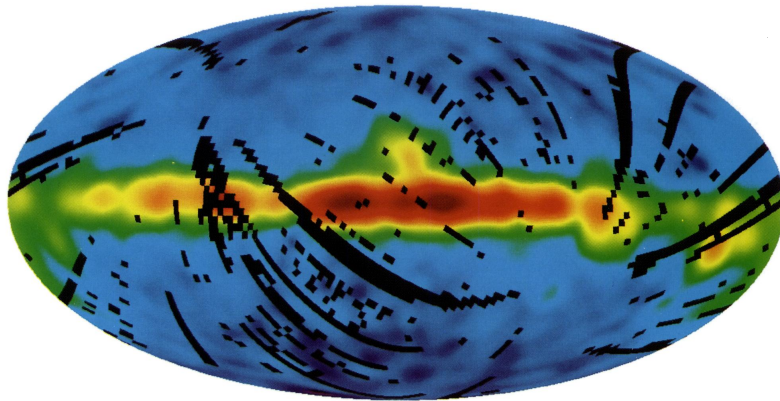
- Ionized gas lanes are less well understood than neutral ones, owing to fewer high spectral and spatially resolved maps of ionized gas tracers.
- [NII] and [CII] as tracers of ionized gas
 - I.P. of C is 11.1 eV, so it is readily ionized by ISM UV ($\lambda > 912 \text{ \AA}$)
 - [CII] emits in weakly & highly ionized components; WIM, HI clouds, Diffuse H_2 clouds w.o. CO, HII regions, PDRs
 - I.P. of N is 14.5 eV, photoionized by FUV ($\lambda < 912 \text{ \AA}$), collisional ionization by electrons ($T_k > 6000\text{K}$), and charge exchange with H^+ ($T_k > 5000\text{K}$)
 - [NII] only arises from highly ionized components: WIM, HII regions, Ionized Boundary Layers.





COBE FIRAS [CII] & [NII] Surveys

COBE FIRAS 158 μm C⁺ Line Intensity



COBE FIRAS 205 μm N⁺ Line Intensity

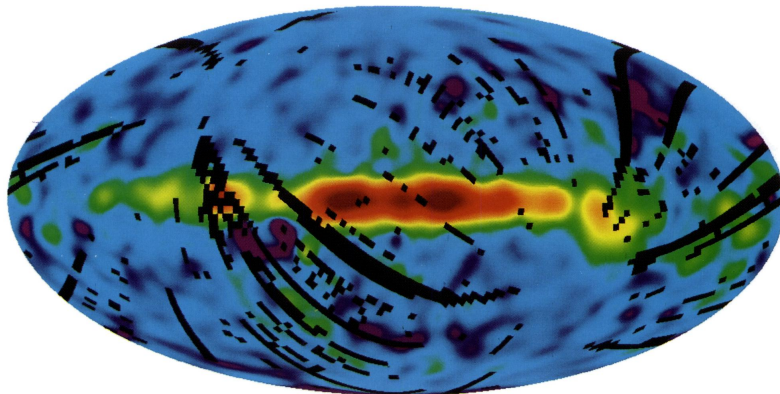


FIG. 1.—Maps are projections of the full sky in Galactic coordinates. The plane of the Milky Way is horizontal in the middle of the map with the Galactic center at the center. Galactic longitude $l = 90^\circ$ is left of center. Maps are smoothed to 10° resolution. *Top*: Full sky map of $158 \mu\text{m}$ C⁺ emission from the COBE FIRAS experiment. *Bottom*: Full sky map of $205 \mu\text{m}$ N⁺ emission from the COBE FIRAS experiment.

BENNETT et al. (see 434, 591)

Bennett et al. (1994)

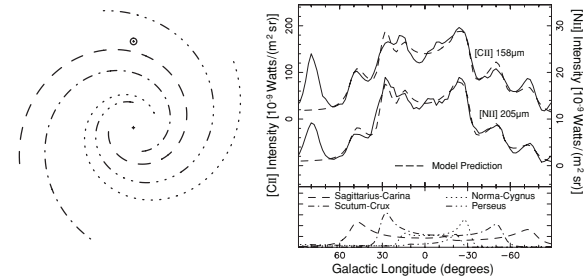
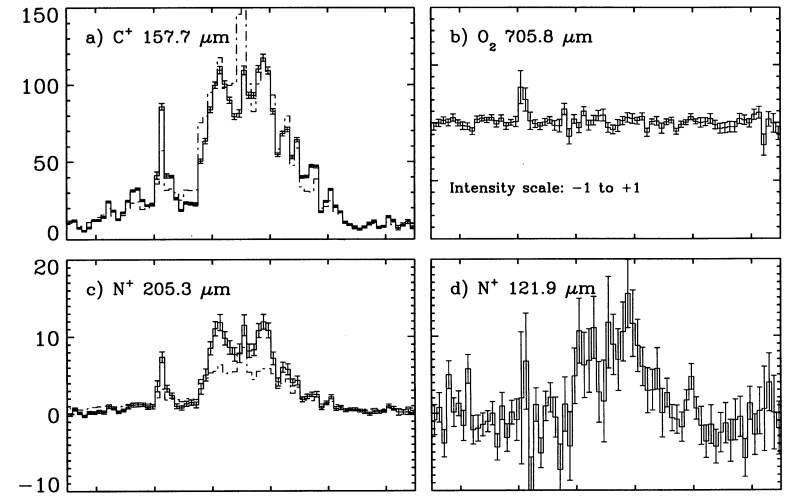


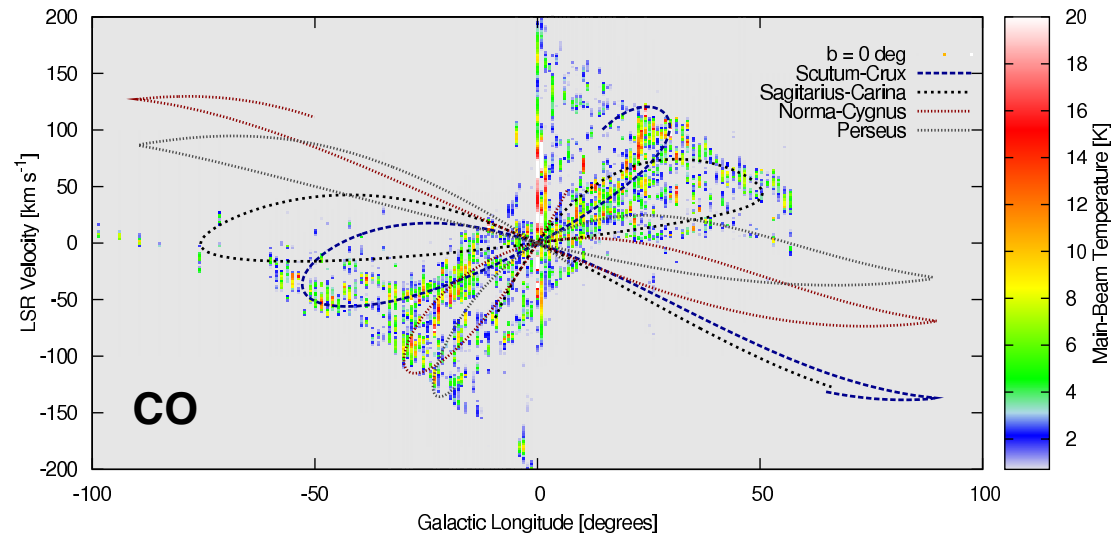
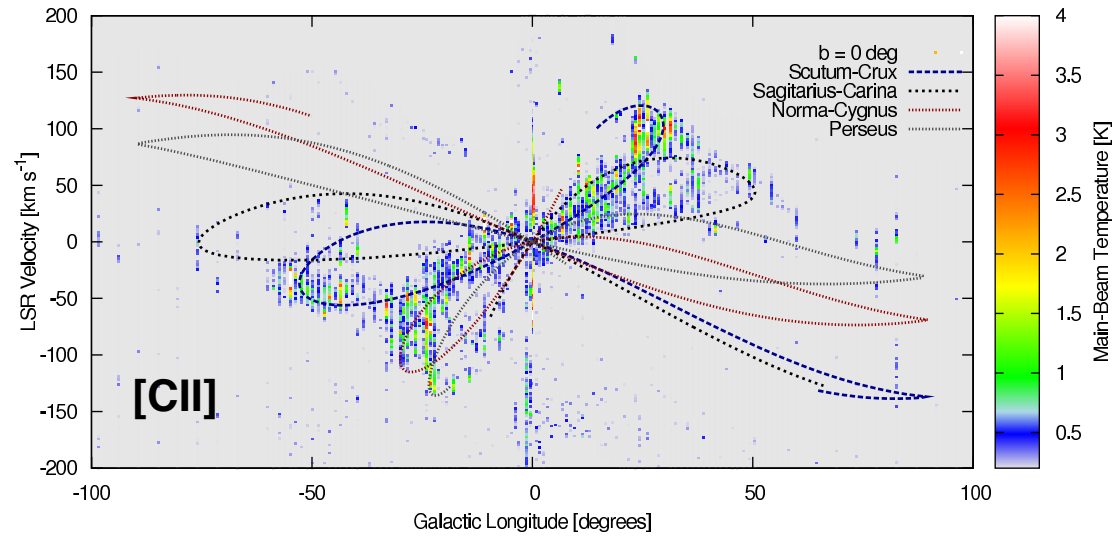
Figure 8. Left: geometry of the four-arm model providing the best fit to the *FIRAS* line intensities in the Galactic plane. Right top: observed (solid) and predicted (dashed) line intensities along the Galactic plane for this model. Physical parameters for the model are provided in Tables 3 and 4. Right bottom: contributions from each individual arm to the full [CII] intensity curve shown at top (results for [NII] are similar). Line styles link intensity contributions with the individual arms at left and are labeled with traditional names (see Figure 9).

Steiman-Cameron et al. (2010) fit a 4-arm spiral model to the FIRAS data



Herschel GOT C+ [CII] Sparse Survey

Herschel OTKP GOT C+
Survey [CII] \approx 500 LOS
(Pineda et al. 2013;
Langer et al. 2014)



[CII] and CO ($b = 0^\circ$) trace spiral arms (Pineda et al. 2013)



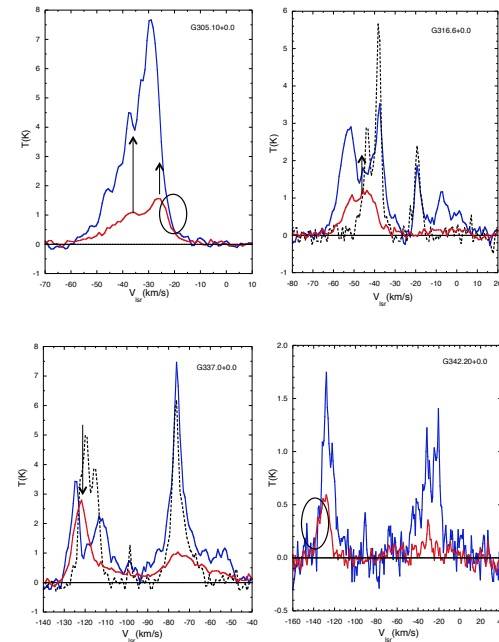
Herschel HIFI [NII] Galactic Survey



No velocity resolved *Herschel* N⁺ Galactic Sparse Survey

Only a sparse PACS 205 and 122 micron survey of about 140 GOT C+ LOS

And 10 HIFI [NII] 205 micron GOT C+ LOS (see Langer et al. 2016)





Herschel [NII] PACS Galactic Survey

THE ASTROPHYSICAL JOURNAL, 814:133 (21pp), 2015 December 1

(Goldsmith et al. 2015)

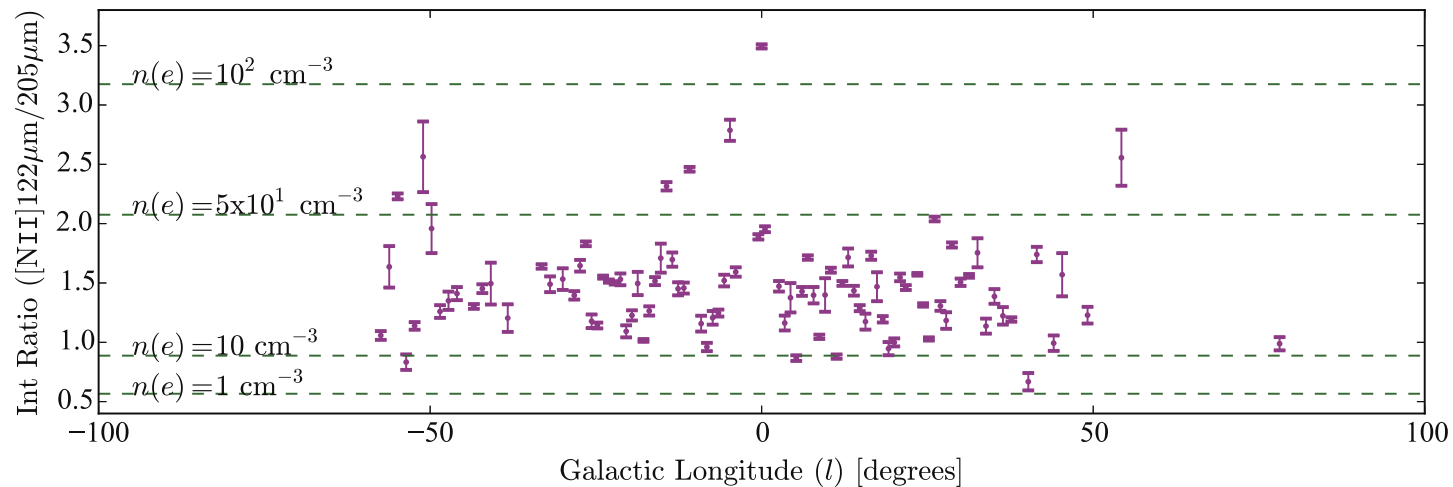


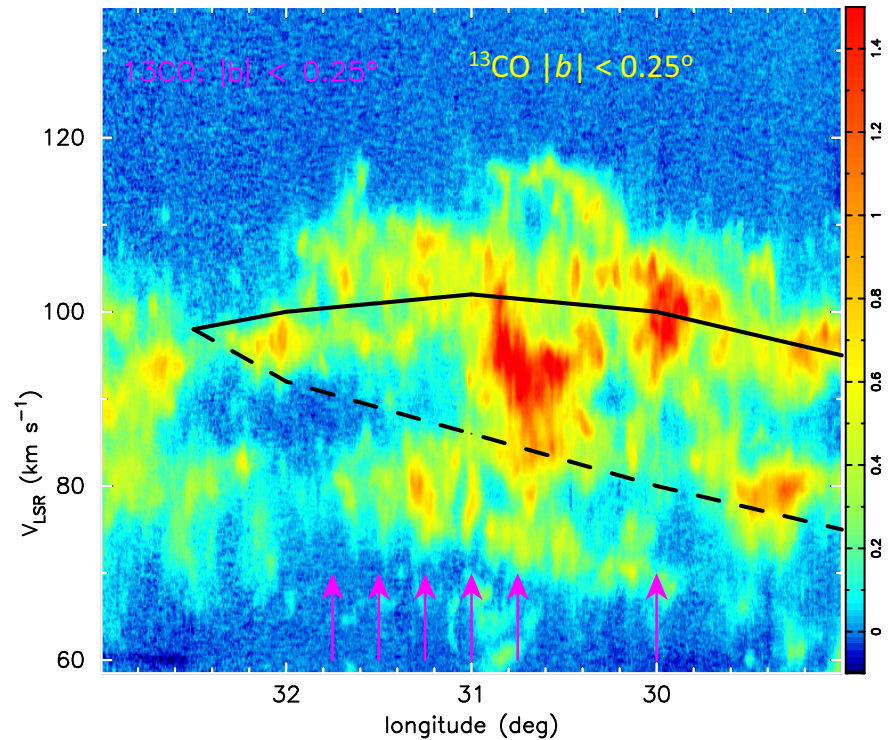
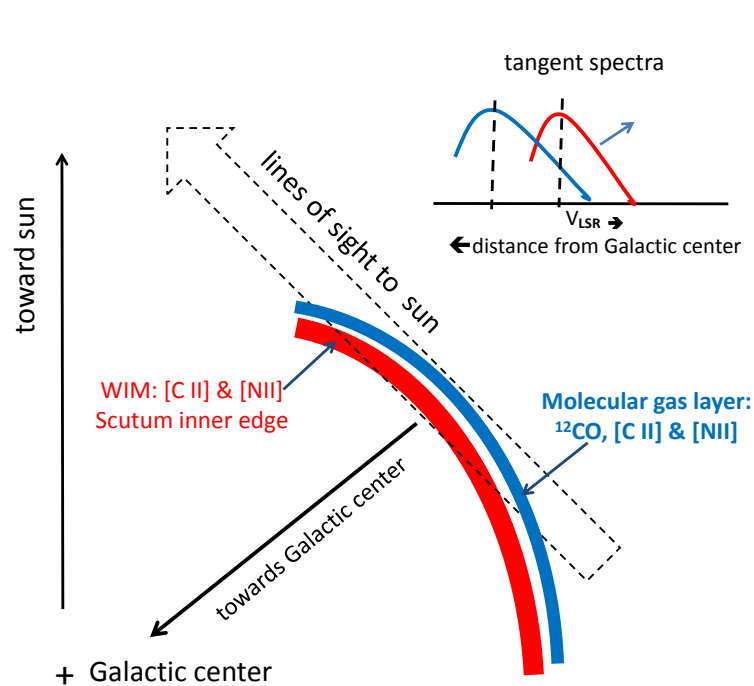
Figure 19. Observed intensity ratio of the two [N II] fine structure lines and derived electron densities are plotted as a function of Galactic longitude.

- Herschel OT2 [NII] PACS Survey (Goldsmith et al. 2015)
 - 140 GOT C⁺ LOSs at $b=0^\circ$ observed in [NII] 205 μm and 122 μm with PACS
- $n(e)$ from [NII] excitation model is high $\approx 10\text{--}50 \text{ cm}^{-3}$ throughout inner Galaxy
- Traditional view - [NII] comes from diffuse WIM or dense HII regions
- PACS and HIFI Galactic plane survey indicate it is more complicated



Scutum Arm Tangency

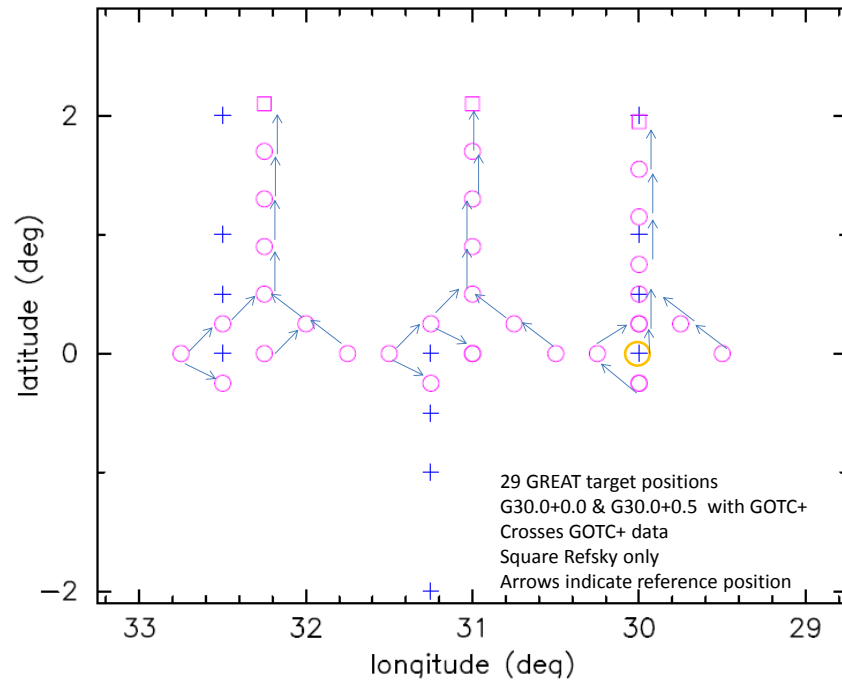
- 1) Tangency allows for separation of gas layers across the arm.
- 2) The detection of weak emission due to long path length.
- 3) Study of the evolution of the gas from ionized low density to neutral high density.



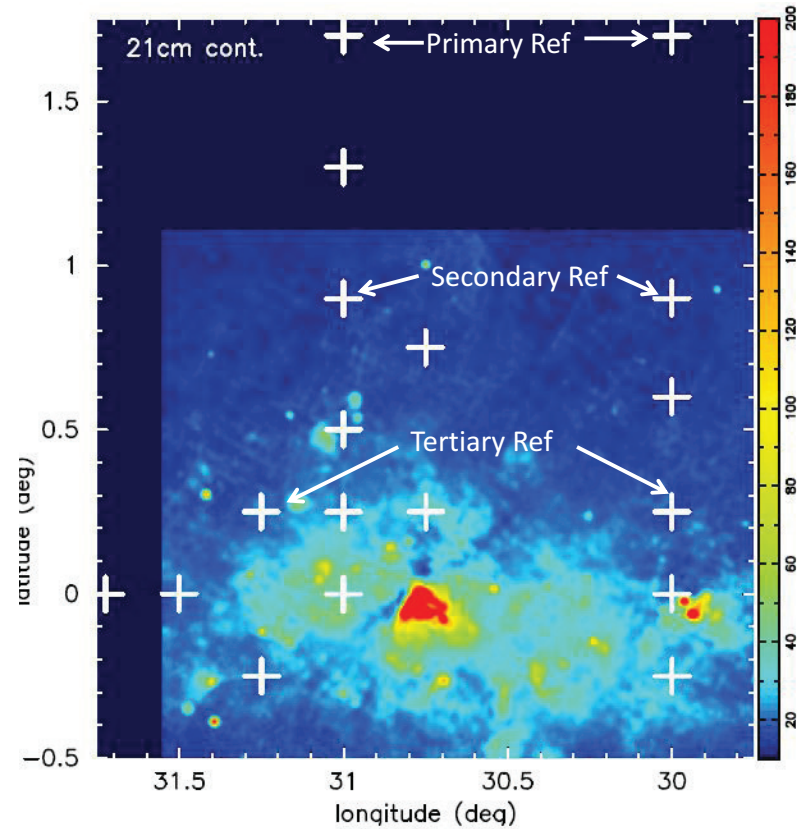
^{13}CO I - V plot of Scutum arm at $b = 0^\circ$ (GRS Survey Jackson et al. 2006.)
Inner (black solid) and outer (black dashed) lines mark the tangencies (from Reid 2016).
The arrows at the bottom mark the LOS observed with upGREAT and GREAT



Cycle 4 [NII] & [CII] Scutum Arm Survey



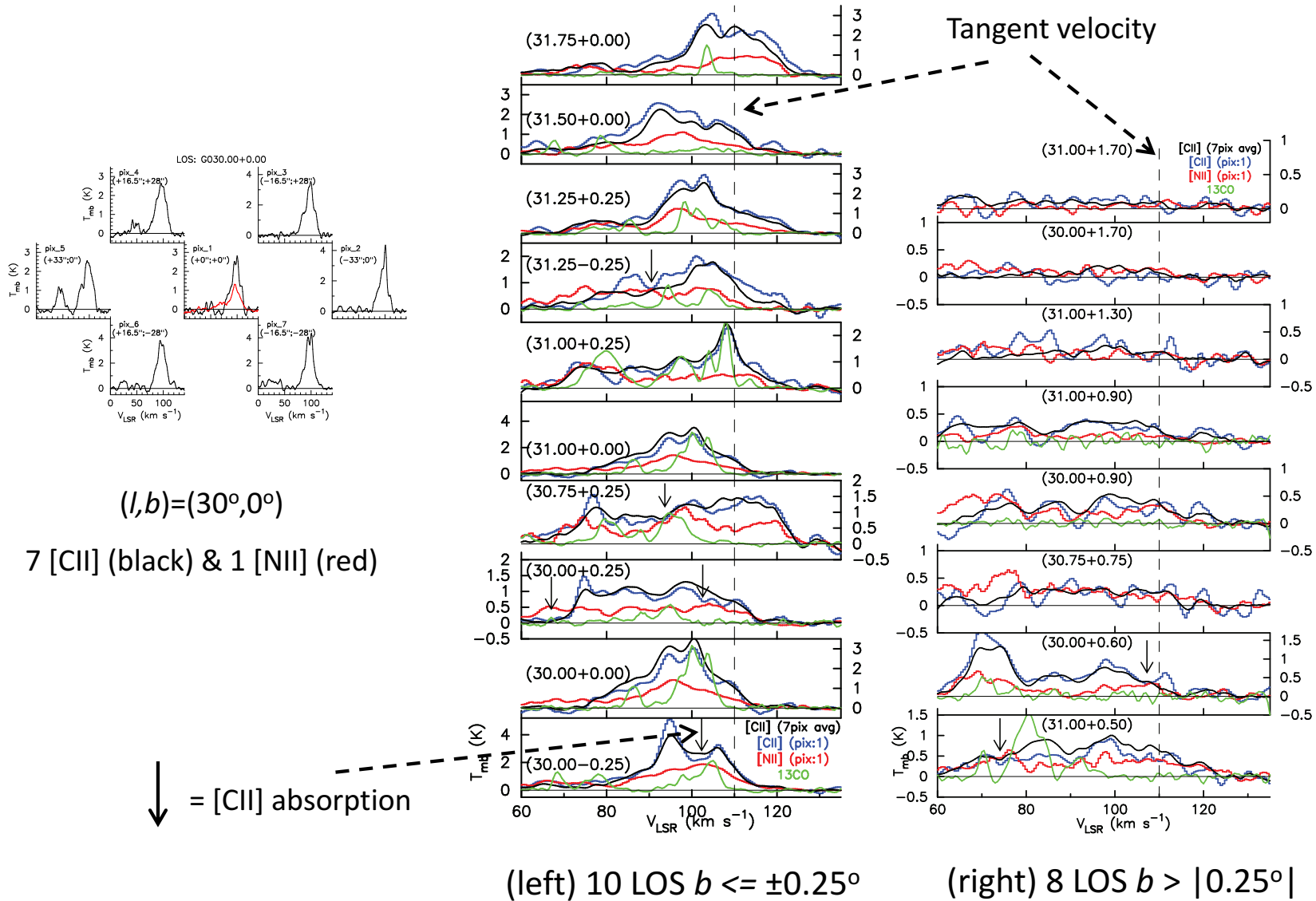
Planned cut across Scutum arm in longitude using *b* scans to calibrate the data



Actual partial map due to insufficient flight time in Cycle 4

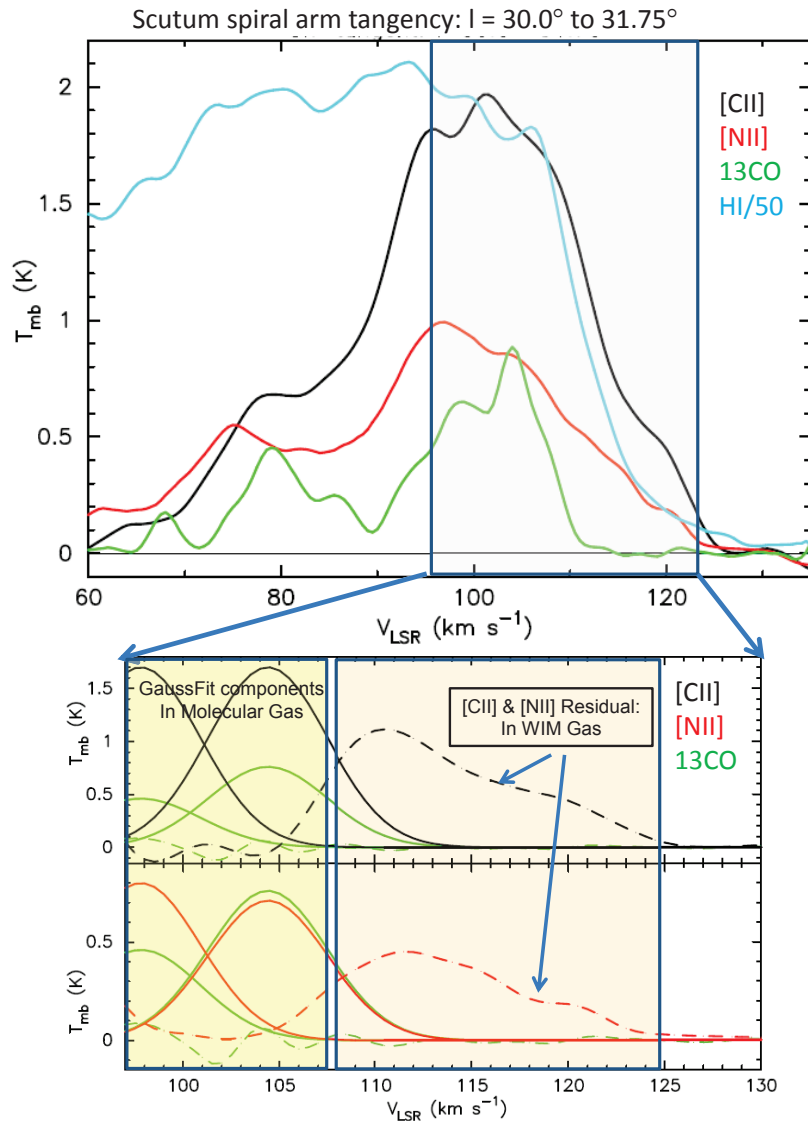


[NII] & [CII] GREAT/upGREAT Observations





Averaged Spectra within $b = |0.25^\circ|$



(Top) Ionized gas tracers extend to much higher V_{LSR} than molecular gas and are located at the leading edge of the arm

(Bottom) Expanded view of ionized gas emission after subtracting out the [CII] and [NII] associated with ^{13}CO .

Subtraction involved a multi-Gaussian fit using ^{13}CO parameters for the V_{LSR} components

For $V_{\text{LSR}} > 110$ km/s the [CII] and [NII] excess arise solely from WIM.



$n(e)$ of the Tangent WIM

$$I_{ion}([N II]) = 0.156x_{-4}(N^+)L_{pc}n(e)f_1(n(e), T_k) (\text{K km s}^{-1}), \quad (1)$$

For 3P_1 level $n_{cr}(e) \approx 175 \text{ cm}^{-3}$

At low densities ($n(e) < 11 \text{ cm}^{-3}$) and for $T_k \sim 8000\text{K}$

$$n(e) \approx 18 \left[\frac{I([NII])}{x_{-4}(N^+)L_{pc}} \right]^{0.5}$$

$L = 1 \text{ kpc}$, $T = 8000\text{K}$, $x(N^+) = 1.4e-4$

$[N II]$ in the plane $b < |0.25^\circ|$ $\langle n(e) \rangle \approx 0.9 \text{ cm}^{-3}$

$[N II]$ out of the plane $b > |0.25^\circ|$ $\langle n(e) \rangle \approx 0.4 \text{ cm}^{-3}$



Spiral Arm WIM vs. Interarm WIM

Interarm WIM

- 1) highly ionized gas, $x(\text{H}^+) \approx 1$,
- 2) low density $n(e) \approx 0.02 - 0.10 \text{ cm}^{-3}$
- 3) high temperature, $T_{\text{kin}} \approx 6,000 - 10,000\text{K}$
- 4) fills a 2 – 3 kpc layer around the midplane
- 5) large filling factor

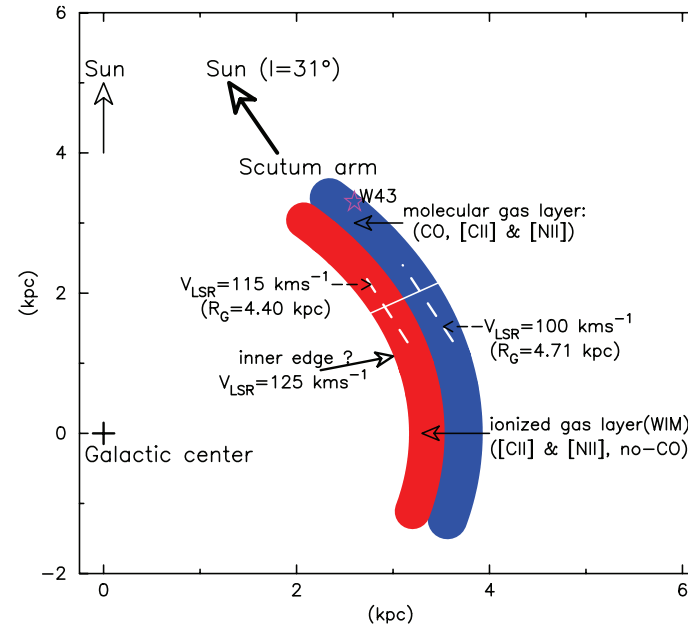
Scutum tangency WIM

$n(e) \approx 10 \times$ larger than interarm WIM within $b = \pm 0.25^\circ$



WIM Dynamics Along the Tangency?

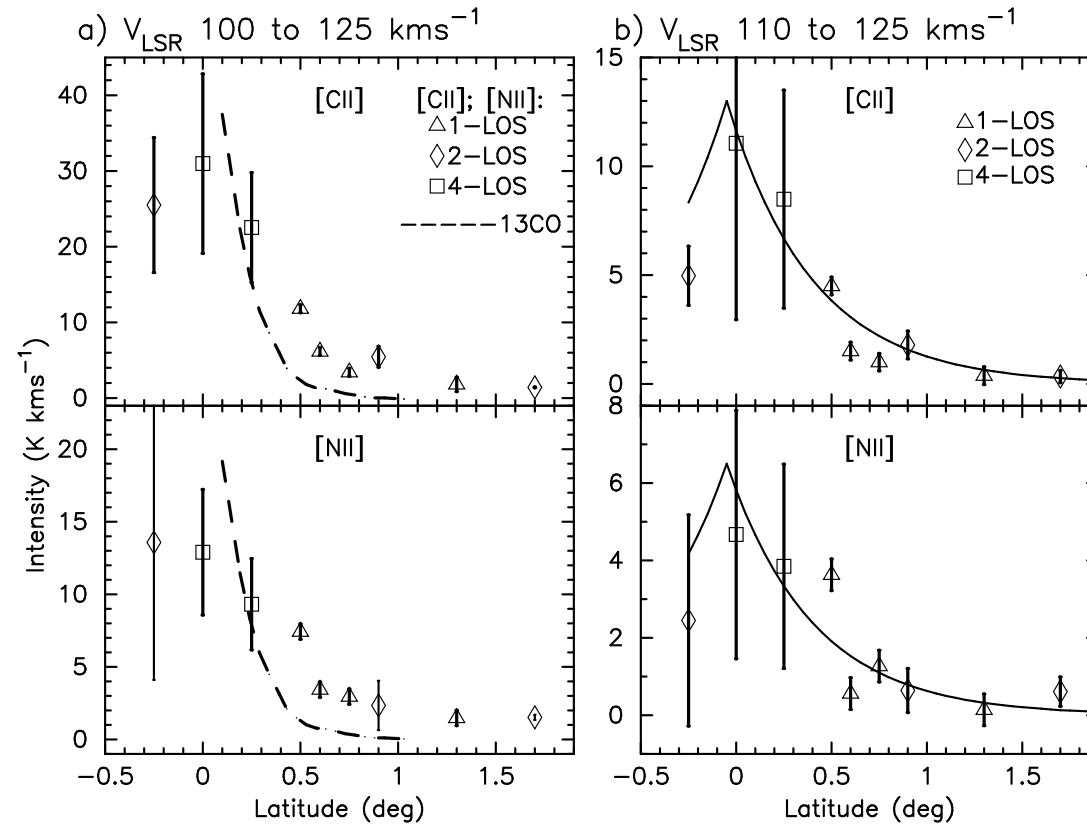
Schematic radial cross section of spiral arm perpendicular to LOS to tangency (not to scale).



The increased density of the WIM along the tangency is likely due to compression of interarm WIM in the gravitational potential of the leading edge of the inner spiral arm.



[CII], [NII], & ^{13}CO Scale Heights



(left) There is a sharp the drop in ^{13}CO is compared to [NII] & [CII] by $b = 0.5^\circ$ – smaller scale height. (right) There is no measurable ^{13}CO and the [CII] & [NII] arise solely from the WIM. The fit is given by $\exp(-(b-\delta b)/b_0)$ with $\delta b = -0.05^\circ$ and $b_0 = 0.45^\circ$.



Ionized Gas Associated with the Molecular Layer

1) The denser ionized gas is associated with the molecular gas deep inside the arm.

As indicated by [NII] associated with ^{13}CO gas at $V_{\text{LSR}} < 110$ km/s.

2) This [NII] is widespread throughout the Scutum spiral arm tangency with typical intensity

$$I([\text{NII}]) \approx (0.35 - 0.50) I([\text{CII}])$$

Much larger than the 0.1 to 0.2 ratio found by COBE FIRAS to be typical of the Galactic distribution

3) Furthermore, the z-scans show that [NII] is strongest at the midplane where the dense molecular cloud tracer ^{13}CO peaks



Dense Ionized Gas and the Molecular Layer

PACS survey observed two Scutum LOS

$$(30.0^\circ, 0^\circ) \langle n(e) \rangle = 29 \text{ cm}^{-3} \text{ and } N(N^+) = 7.7e16 \text{ cm}^{-2}$$

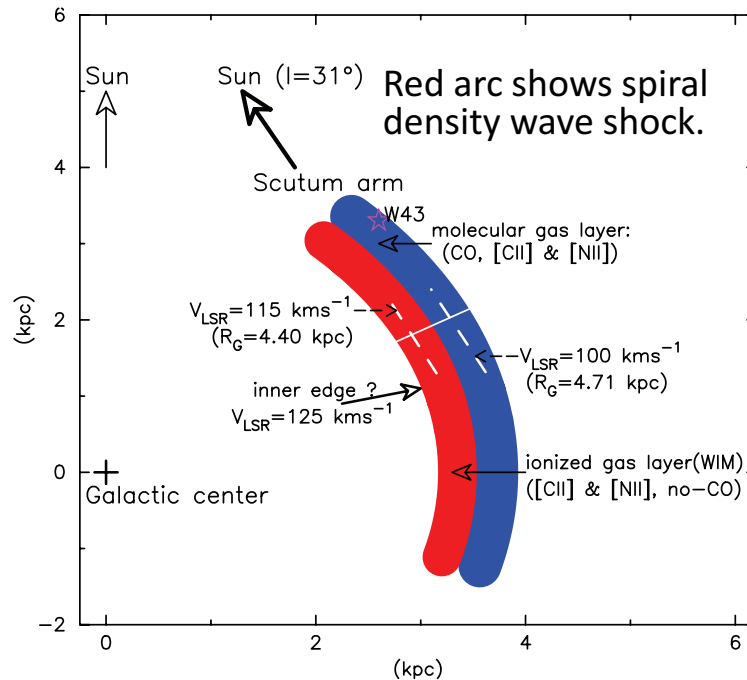
$$(31.28^\circ, 0^\circ) \langle n(e) \rangle = 31 \text{ cm}^{-3} \text{ and } N(N^+) = 11.4e16 \text{ cm}^{-2}$$

Strong [NII] emission was detected all across the PACS 25 element array (45") corresponding to about 1.5 pc - evidence of broadly distributed [NII] emission.

SOFIA observations show [NII] 205 μm emission associated with ^{13}CO comes from across the arm and thus likely traces the high density ionized gas found by Goldsmith et al. (2015).



Source of Dense Ionized Gas?



HII or Ionized Boundary Layers?

Suggestion: Most of the [NII] is due to shock compression of the WIM as it flows onto the denser neutral gas.

The gravitational potential of the arm can accelerate the WIM over a few hundred pc to several km/s, much greater than the sound speed in the neutral clouds (about 1 km/s), resulting in a shock at the interface.

This general mechanism would explain the high $n(e)$ densities at widely distributed LOS in the inner Galaxy seen in the Goldsmith et al. (2015) PACS survey.



Side Note: Nitrogen to Carbon Ratio in the WIM

[CII] and [NII] in the WIM can be used to derive the N/C abundance ratio because there is no other ISM component contributing to [CII] along the LOS

$$x(N^+ / C^+) = 0.675 \frac{f_{3/2}(C^+) I_{10}([NII])}{f_1(N^+) I_{3/2}([CII])}$$

$$x(N^+ / C^+) = 1.168 \frac{I_{10}([NII])}{I_{3/2}([CII])}$$

$$\langle I([NII])/I([CII]) \rangle_{WIM} = 0.37 \text{ all LOS with } b < |0.25^\circ|$$

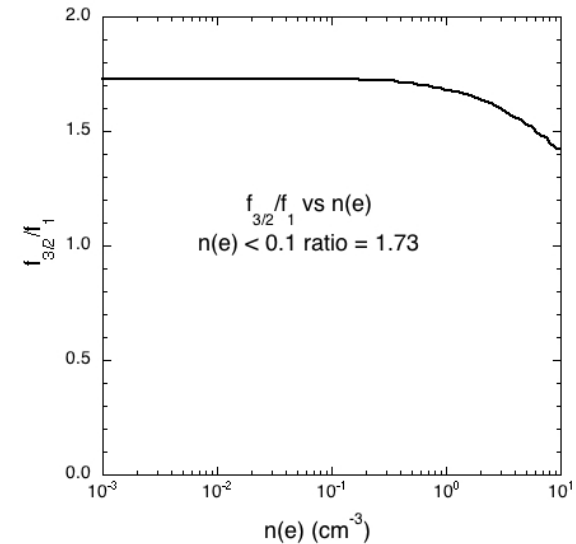
$$x(C^+)/x(N^+) = 2.3$$

$$x(N^+)_{\odot} = 6.75e(-5) \text{ (Asplund et al. 2009)}$$

$$x(C^+)_{\odot} = 1.40e(-4) \text{ (Cardelli et al. 1996)}$$

$$x(C^+)_{\odot} = 1.61e(-4) \text{ (Sofia et al. 2004)}$$

$$x(C^+/N^+)_{\odot} = 2.1 - 2.4$$





Summary

- Observed [NII] and [CII] in the Scutum Arm tangency
- Found compressed WIM and high density $n(e)$
- High density N^+ implies shock compression
- More extensive mapping of [NII] 205 μm across the spiral arm tangencies is needed to elucidate the interaction of the spiral arm potential with the interarm gas.
- Large scale maps of [CII] are beginning to emerge from SOFIA
- Ultimately, we need similar maps of [NII], enabled by large heterodyne arrays, to get a complete picture of the ISM and Galactic evolution